ISSN 1087-6596, Glass Physics and Chemistry, 2015, Vol. 41, No. 5, pp. 503–508. © Pleiades Publishing, Ltd., 2015.

The Size-Effect of Al_2O_3 on the Sinterability, Microstructure and Properties of Glass-Alumina Composites[1]

Bo Li, Yang Xu, and Shuren Zhang

State Key Laboratory of Electronic Thin Films and Integrated Devices, School of Microelectronics and Solid-State Electronics, University of Electronic Science and Technology of China, Chengdu, 610054 China

e-mail: lbuestc@163.com

Received June 16, 2014

Abstract—The glass-ceramic composites were prepared from low-softening glass $CaO–B_2O_3–SiO_2$, micrometer and nanometer alumina. The influences of nano-Al_2O_3 on the sinterability, microstructure, dielectric property, mechanical strength, and thermal expansion of glass-alumina composites were investigated. The densification mechanism of nano-Al_2O_3 modified glass-alumina composites was revealed further. The results show that nano-Al_2O_3 effectively lowers the densification temperature of glass-alumina ≤900°C. The density gradually increases with increasing nano-Al_2O_3 to 15 wt %, and then decreases. Dielectric constant, dielectric loss, and flexural strength respectively versus nano-Al_2O_3 exhibit a similar change trend to the density. The sample with 15 wt % nano-Al_2O_3 sintered at 900°C could form the dense microstructure (~2.95 g/cm^3) and achieve the high performance: low dielectric constant (6.13), low dielectric loss (5.2×10^{-4}), low thermal expansion (4.21×10^{-6}/°C), and high mechanical strength (178 MPa).

Keywords: alumina, glass-ceramic composites, low temperature cofired ceramic (LTCC), nanometer

DOI: 10.1134/S1087659615050041

INTRODUCTION

To meet the demands of very large scale integration (VLSI), the low temperature cofired ceramic (LTCC) technology for advanced electronic packages quickly developed during the last decades [1, 2]. In fact, several approaches including glass-ceramics [3, 4] and glass-ceramics composites [5–8] have been designed and reported in the literature since 1990s. The latter approach can provide a high degree of flexibility in designing materials with a combination of electrical, thermal and mechanical properties. Glass-alumina composites, which consist of borosilicate glass and alumina, are expected as hopeful substrate materials for integrated circuits (IC), because they can be densified at low temperatures and can get the properties of low dielectric constant and thermal expansion coefficient close to that of silicon [6, 7]. Authors [6] studied the effect of alumina particle size on the crystallization, thermal and dielectric behavior of glass composite. Recently, authors [7] reveal that many aspects such as sinterability, microstructure and dielectric properties of glass-alumina composites were strongly influenced by varying the alumina content. Moreover, due to the particular characteristics such as the surface effect and small-scale effect, nanopowder has been widely employed to improve the characters for other materials [9]. However, the influence of Al_2O_3 nanopowder on such glass-alumina system has not been reported until now. In this paper, we report a low-temperature-fired nano-Al_2O_3-modified glass–alumina composite with good performances, including low dielectric constant, low thermal expansion, and high mechanical strength, used in electronic devices. Especially, the effects of nanometer Al_2O_3 on the sinterability, microstructure as well as dielectric properties, flexural strength and thermal expansion of glass–alumina composites are discussed in detail.

EXPERIMENTAL PROCEDURE

A low-softening borosilicate glass system $CaO–B_2O_3–SiO_2$ (CBS) adopted here was synthesized by the sol-gel method [4]. Two kinds of pure alumina powders were used in this study, that is, coarse powder and nano-powder, respectively, with a particle size range of 0.2–0.7 μm and 20–70 nm, as shown in Figs. 1a and 1b. The powder mixture, containing the required amounts of glass and alumina as given in Table 1, was ball-milled in alcohol for 24 h. After dried and sieved, the powders mixed with 5 wt % PVA were uniaxially pressed into compacts at 20 MPa. After binder burnout at 450°C, the green compacts were then sintered at the temperature 800–950°C for 2 h in air.

---

[1] The article is published in the original.

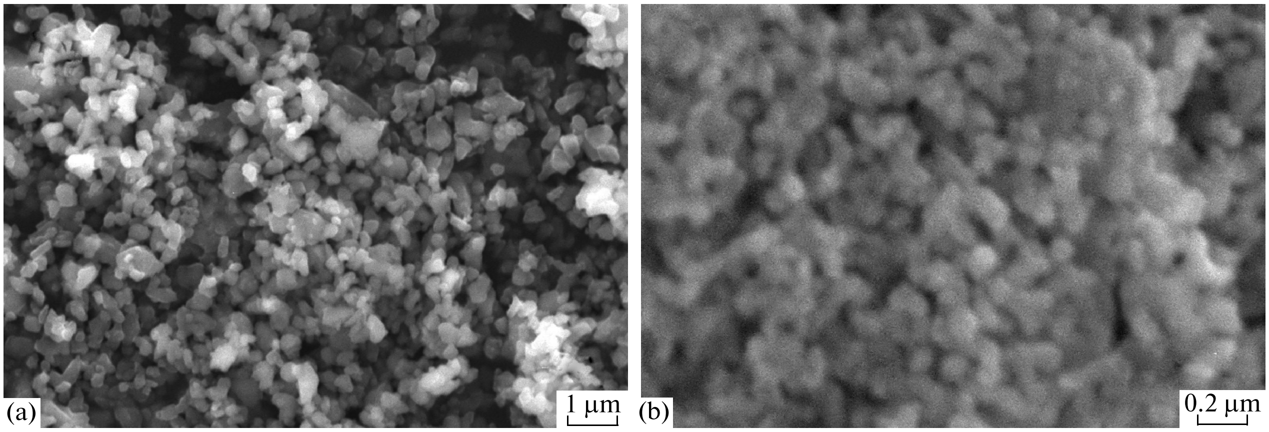

Fig. 1. SEM micrographs of Al_2O_3 raw materials: a—coarse powder, b—nanopowder.

The bulk density of as-fired samples was measured by the precision density balance (AND GF-300D) based on the Archimedes method. The microstructure was observed by the scanning electron microscope (SEM, HITACHI S-530). The dielectric properties (ε and $\tan\delta$) at 1 MHz were tested by the Agilent precision 4284A LCR meter. The flexural strength was measured by the electronic universal testing machine (SANS CMT6104). The thermal expansion coefficient (TEC) in the temperature range from room temperature to 400°C at a heating rate of 5°C/min was conducted using the dilatometer system (NETZSCH DIL 402PC).

RESULTS AND DISCUSSIONS

Figure 2 shows the relationship between the bulk density and the sintering temperature for samples with various nano-Al_2O_3 contents. The density of glass-ceramics gradually increases as the firing temperature increasing from 800 to 900°C. After reaching a maximum value at 900°C, the densities of samples significantly decrease with the increase of sintering temperature from 900 to 950°C. This phenomenon is due to the overfiring of composites as well as the expansion of close pores above 900°C [10]. Thus, nano-Al_2O_3 effectively lowers the densification temperature of glass–ceramics to 900°C. Moreover, the sintering behavior of composites strongly correlates with the amount of nano-Al_2O_3. At a given sintering temperature, the density enhances gradually and then decreases when the nano-Al_2O_3 content increases. Sample 4 with 15 wt % nano-Al_2O_3 sintered at 900°C shows the highest desity (2.95 g/cm^3). Besides, the density increases with increasing the sintering temperature, which indicates the sample 7 with 50 wt % nano-Al_2O_3 still needs a higher temperature to complete its densification.

Table 1. Compositions of various glass-ceramic

Samples	CBS-glass, wt %	Al_2O_3 (wt %)	
		coarse powder	nanopowder
0	50	50	0
1	50	47.5	2.5
2	50	45	5
3	50	40	10
4	50	35	15
5	50	30	20
6	50	25	25
7	50	0	50

To further investigate the sintering behavior, the microstructural change of the sintered composites was analyzed by SEM. Figure 3 displays the micrographs of composites with different amounts of nano-Al_2O_3 sintered 900°C. Samples 1, 2 with 2.5 and 5 wt % nano-Al_2O_3 have loose microstructures with a few pores and voids. The sintered compacts become denser with the increase of nano-Al_2O_3 in the range from 2.5 to 15 wt %, as shown in Figs. 3a–3c. Specifically, the sample 4 with 15 wt % nano-Al_2O_3 shows a dense microstructure, since the glass phase is integrated with ceramic phase closely. Simultaneously, the cross-section of SEM micrograph for the sample 4 is shown in Fig. 4. Fewer pores and microcracks are observed inside the sintered body. In general, for partially reactive systems such as BSG + alumina, the dissolution of the ceramic filler Al_2O_3 in BS glass is localized and limited, and no particle growth and shape accommodation are observed. However, 25 and 50 wt % nano-Al_2O_3 doped samples 6, 7 reveal large irregular shaped grains with pores and microcracks embedded in the glass-ceramic matrix (see Figs. 3d–3e). The abnormal grain growth could result from the higher activity of nano-Al_2O_3 and the liquid sintering. It is considered that the internal pores and microcracks are originated from the agglomeration of nano-Al_2O_3 powders. Accordingly, the result of densification is also confirmed by the microstructural observation.

The densification of glass-ceramic composites can be described by the conventional three-stage liquid phase sintering i. e. particle rearrangement, dissolution and precipitation, and solid state sintering [5]. Depending upon the reactivity between glass and ceramic, the densification of glass + ceramic can be further classified as nonreactive (BSG + cordierite), partially reactive (BSG + alumina), and completely reactive systems (BSG + high silica glass) [5–8]. The densification mechanism of nano-Al_2O_3 modified glass/alumina composites can be explained as follows. A proper amount of nano-Al_2O_3 (15 wt %) can uniformly disperse in the glass-ceramic matrix during the procedures of ball-milling and sintering. Further, nano-Al_2O_3 particles can fill in the voids of the coarse Al_2O_3 compacts. Above the softening point (~785°C [4]), CBS glass becomes a viscous liquid and holds Al_2O_3 particles together. Moreover, due to the large specific area of Al_2O_3 nanopowders, the increased interface benefits the ion diffusion and mass transfer during the solid state sintering. The extremely high surface activity of nano-Al_2O_3 also promotes the firing process. In addition, the diffusion of aluminum ions into the glass matrix could form the liquid phase and lower the firing temperature.

The dielectric properties of different samples as a function of nano-Al_2O_3 content are shown in Fig. 5. With the increase of nano-Al_2O_3, the dielectric constant (ε) increases steadily, and then declines dramatically at above 20 wt % of nano-Al_2O_3. On the contrary, the dielectric loss (tanδ) changes slightly when nano-Al_2O_3 less than 20 wt %, and then enhances significantly. These changes suggest that the dielectric properties are seriously dependent on the composition, density and microstructure. As we know, a lower dielectric constant of substrate is desired for allowing the high-speed signal to propagate with a shorter delay in large-scale integrators (LSI). Although the lowest ε value (~4.3) is achieved at 50 wt % nano-Al_2O_3, the rather bad tanδ value ($\sim 10^{-2}$) is obtained at the same time, which is attributed to the presence of porosity and microcracks. As for the dielectric properties, the amount of nano-Al_2O_3 should thus be controlled within 20 wt % in this system.

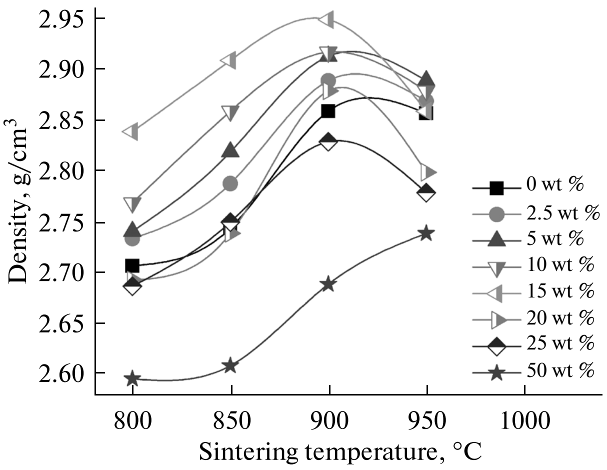

Fig. 2. Bulk densities of various samples as a function of sintering temperatures.

Figure 6 shows the flexural strength of glass/ceramic composites versus nano-Al_2O_3 addition. The flexural strength increases gradually and reaches the maximum of 178 MPa as nano-Al_2O_3 increases to 15 wt %. A further increase in nano-Al_2O_3 ≥ 20 wt % will give rise to a huge reduction in the flexural strength. This trend of the flexural strength versus nano-Al_2O_3 contents agrees well with that of the bulk density mentioned above. The reasons for an increase in the flexural strength maybe include three aspects. First, it is mainly attributed to the enhancement of densities and the elimination of pores because of the doping effect of nano-Al_2O_3. Second, the development of α-Al_2O_3 grains and the crystallization of CBS glass can also improve the flexural strength of glass-ceramic. Third, the combination of glass and ceramic becomes stronger, because the interface between two different phases is modified by the diffusion of nano-Al_2O_3. In addition, the decrease in flexural strength for samples with higher contents of nano-Al_2O_3 (≥20 wt %) could be due to the formation of many pores or microcracks resulted from the severe agglomeration of nano-Al_2O_3 powders.

In addition to electrical and mechanical properties, TEC is another critical parameter for the substrate application. Figure 7 draws the thermal expansion curves of composites with various nano-Al_2O_3 contents. Both the magnitude of relative expansion and the slope of curves change clearly by varying the amount of nano-Al_2O_3. TEC data calculated from Fig. 7 are summarized in Table 2. TEC slightly fluctuates around $4.21–4.97 \times 10^{-6}$/°C for 0–20 wt % nano-Al_2O_3, and then increases to $5.14–5.83 \times 10^{-6}$/°C for 25–50 wt % nano-Al_2O_3, which is associated with the different microstructures and densities of samples. Lower TEC values are obtained for all samples with 50 wt % of alumina, which is in consistent with the previous result ($4.5–4.6 \times 10^{-6}$/°C) reported in [7].

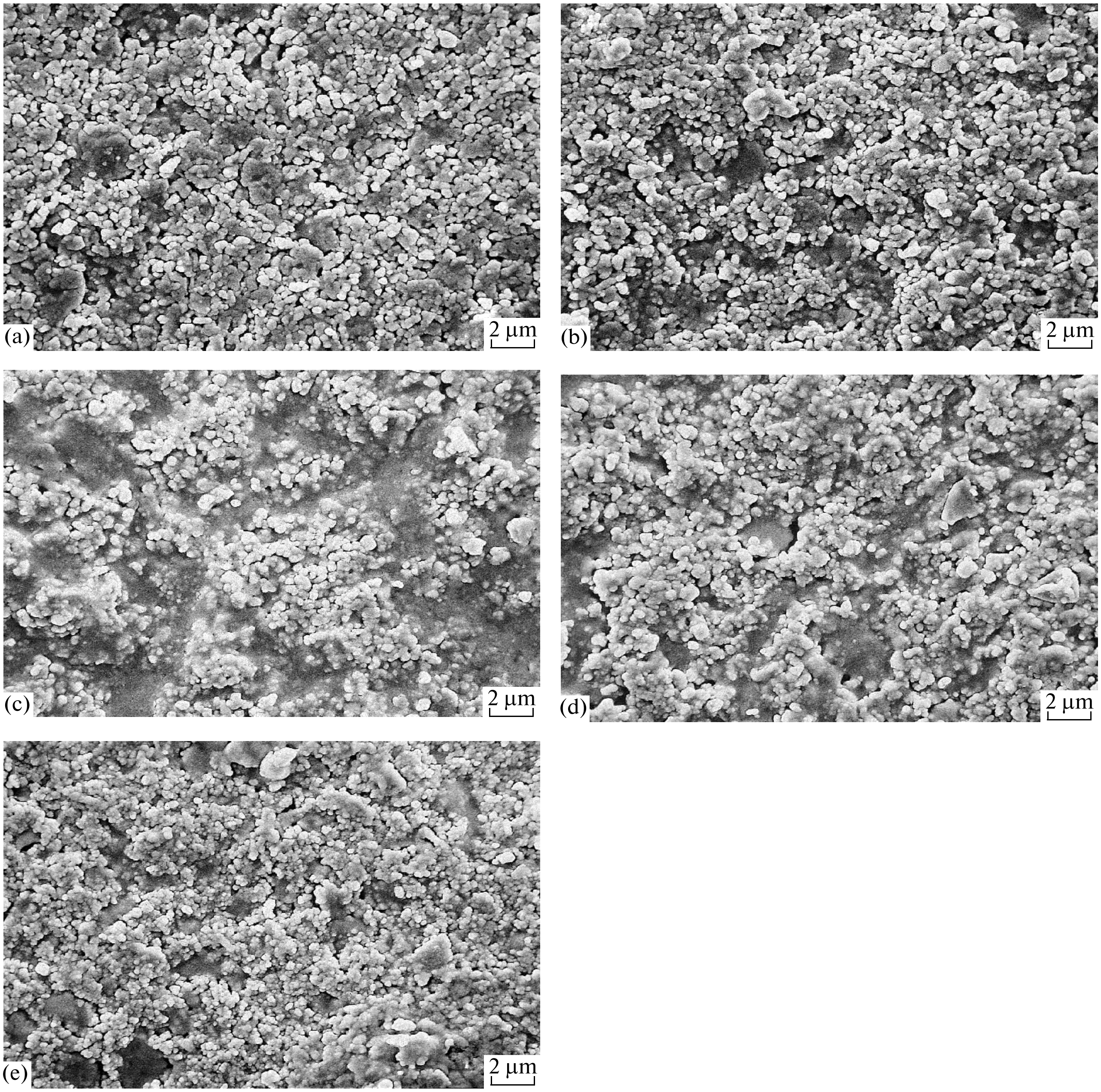

Fig. 3. SEM micrographs of glass-alumina composites sintered 900°C.
(a) 2.5, (b) 5, (c) 15, (d) 25, (e) 50 wt % nano-Al_2O_3.

The formation of cristobalite phase with large TEC in glass-alumina composites can be prevented by increasing alumina content, by which the diffused alumina ions change the structure of glass. To prevent thermal stresses caused by the thermal expansion mismatch, TEC of substrate should be close to that of sil-

Table 2. Experimental values of thermal expansion coefficient

	Samples							
	0	1	2	3	4	5	6	7
Nano-Al_2O_3, wt %	0	2.5	5	10	15	20	25	50
TEC × 10^{-6}/°C	4.86	4.79	4.53	4.97	4.21	4.58	5.14	5.83

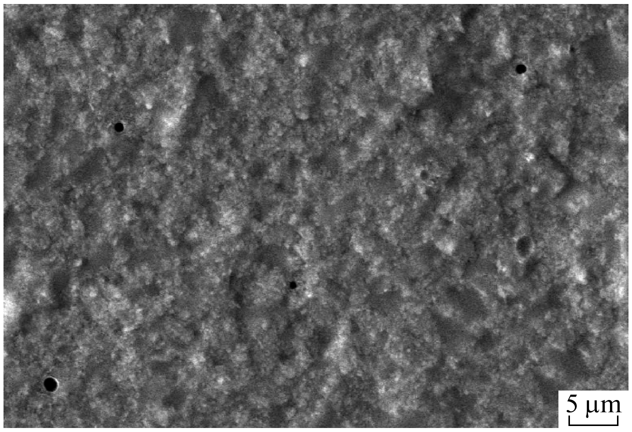

Fig. 4. SEM micrographs for section of composite with 15 wt % nano-Al_2O_3 sintered 900°C.

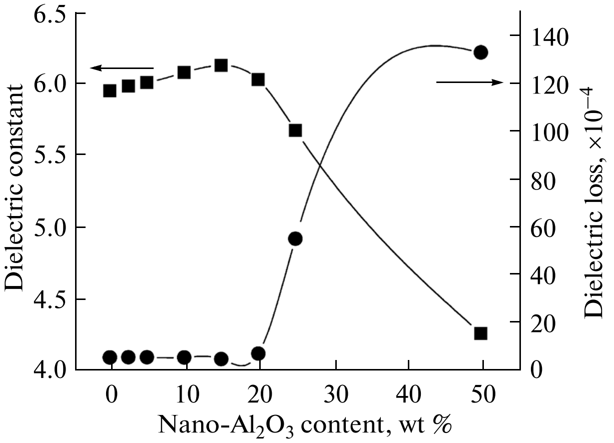

Fig. 5. Dielectric constant (*1*) and dielectric loss of different samples (*2*) as a function of nano-Al_2O_3 content (1 MHz).

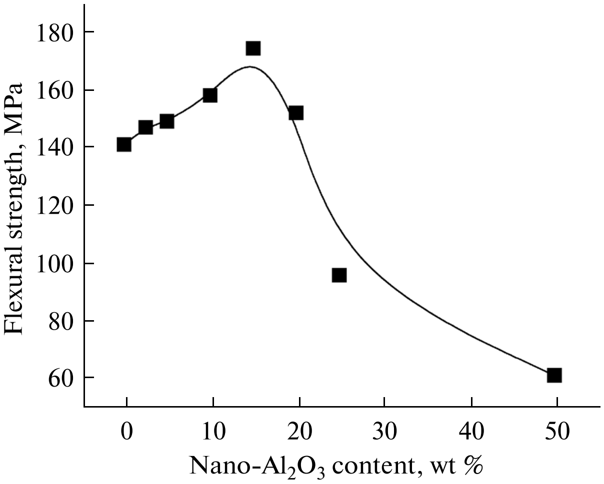

Fig. 6. Flexural strength of glass-ceramics as a function of nano-Al_2O_3 content.

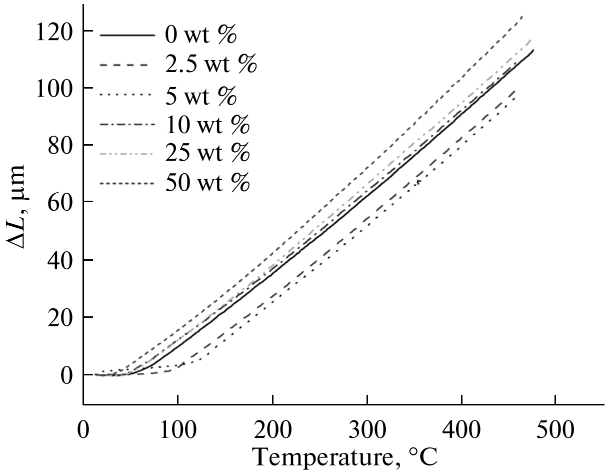

Fig. 7. Thermal expansion curves of different glass-alumina composites.

icon chip (3.5×10^{-6}/°C). Sample 4 with 15 wt % nano-Al_2O_3 shows the lowest TEC of 4.21×10^{-6}/°C. Owing to the formation of microcracks and pores, 50 wt % nano-Al_2O_3 doped composite 7 has a relative higher value of TEC.

CONCLUSION

Due to the higher activity of nanopowder and the liquid phase sintering, nano-Al_2O_3 addition can effectively lower the densification temperature of glass-alumina composites, and the density reaches a maximum value around 900°C. The sinterability, microstructure, dielectric property, flexural strength and thermal expansion of glass-alumina composites are strongly dependent on the amount of nano-Al_2O_3. The bulk density enhances gradually when nano-Al_2O_3 contents increase to 15 wt %, and then decreases. The dielectric constant, dielectric loss, and flexural strength as a function nano-Al_2O_3 show the similar trend to the density. The densification mechanism of nano-Al_2O_3 modified glass/alumina composite is explained as follows: a suitable amount of nano-Al_2O_3 particles (≤15 wt %) can uniformly disperse in the glass-ceramic matrix and fill in the voids of the coarse Al_2O_3 compacts; nano-Al_2O_3 powder with a large specific area can provide the large active interface for the ion diffusion and mass transfer between glass and ceramic, and also promote the reactive sintering process. Moreover, excessive nano-Al_2O_3 (≥20 wt %) will lead to the abnormal grain growth resulted from the higher activity of nano-Al_2O_3 as well as the formation of pores and microcracks originated from the agglomeration of nano-Al_2O_3 powders. 15 wt % nano-Al_2O_3 added glass-alumina composite could be sintered at the low temperature (~900°C), form the dense microstructure (~2.95 g/cm^3), and exhibit the good performances: a low dielectric constant (6.13), a low dielectric loss (5.2×10^{-4}), a low thermal expansion (4.21×10^{-6}/°C), and a high mechanical strength (178 MPa).

REFERENCES

1. Tummala, R.R., Ceramic and glass-ceramic packaging in the 1990s, *J. Am. Ceram. Soc.*, 1991, vol. 74, no. 5, pp. 895–908.
2. Sebastian, M.T. and Jantunen, H., Low loss dielectric materials for LTCC applications: A review, *Int. Mater. Rev.*, 2008, vol. 53, no. 2, pp. 57–90.
3. Knickerbocker, S.H., Kumar, A.H., and Herron, L.W., Cordierite glass-ceramics for multilayer ceramic packaging, *Am. Ceram. Soc. Bull.*, 1993, vol. 72, no. 1, pp. 90–95.
4. Zhou, X., Li, B., Zhang, S., and Ning, H., Effect of Ca/Si ratio on the microstructures and properties of $CaO-B_2O_3-SiO_2$ glass-ceramics, *J. Mater. Sci.: Mater. Electron.*, 2009, vol. 20, no. 3, pp. 262–266.
5. Jean, J.-H. and Lin, S.C., Effect of borosilicate glass on densification and properties of borosilicate glass + TiO_2 ceramic, *J. Mater. Res.*, 1999, vol. 14, no. 4, pp. 1359–1363.
6. Jean, J.-H., Chang, C.-R., Chang, R.-L., and Kuan, T.-H., Effect of alumina particle size on prevention of crystal growth in low-k silica dielectric composite, *Mater. Chem. Phys.*, 1995, vol. 40, no. 1, pp. 50–55.
7. Zawrah, M.F. and Hamzawy, E.M.A., Effect of cristobalite formation on sinterability, microstructure, and properties of glass-ceramic composites, *Ceram. Int.*, 2002, vol. 28, no. 2, pp. 123–130.
8. Jean, J.-H. and Gupta, T.K., Liquid-phase sintering in the glass–cordierite system, *J. Mater. Sci.*, 1992, vol. 27, no. 6, pp. 1575–1584.
9. Li, B., Zhang, S., Zhou, X., Wang, S., and Chen, Z., Preparation of $BaTiO_3$-based ceramics by nanocomposite doping process, *J. Mater. Sci.*, 2007, vol. 42, no. 6, pp. 2090–2096.
10. Monteiro, R.C.C. and Lima, M.M.R.A., Effect of compaction on the sintering of borosilicate glass–alumina composites, *J. Eur. Ceram. Soc.*, 2003, vol. 23, no. 11, pp. 1813–1818.